

# A Saddle-Shaped Expanded Porphyrinoid Fitting C<sub>60</sub>\*\*

Theo Maulbetsch,<sup>[a]</sup> Philipp Frech,<sup>[b]</sup> Marcus Scheele,<sup>[b]</sup> Karl W. Törnroos,<sup>[c]</sup> and Doris Kunz<sup>\*,[a]</sup>

*Dedicated to Professor Gerhard Erker.*

We present the synthesis of a new type of an expanded porphyrinoid macrocycle with a saddle-shaped morphology and its complexation of C<sub>60</sub> guest molecules. The new macrocycle contains four carbazole and four triazole moieties and can be readily synthesized via a copper-catalyzed click reaction. It shows specific photo-physical properties including fluorescence

with a high quantum yield of 60%. The combination of the saddle-shaped geometry with the expanded  $\pi$ -system allows for host-guest interactions with C<sub>60</sub> in a stacked polymer fashion. Evidence for the presence of a host-guest complex is provided both in solution by NMR spectroscopy and in the solid state by X-ray structure analysis.

## Introduction

Expanded,  $\pi$ -extended porphyrins<sup>[1]</sup> and similar macrocyclic  $\pi$ -systems have attractive properties not only in coordination chemistry<sup>[2]</sup> but also in electrochemistry,<sup>[3]</sup> molecular recognition<sup>[4]</sup> and host-guest interaction.<sup>[5]</sup> Large conjugated  $\pi$ -systems with defined structures are often hard to synthesize, with the annulation of the monomeric aromatic moieties being the prevalent obstacle most of the time.<sup>[6]</sup> Additionally, macrocyclization often yields products of different ring sizes that can be hard to separate. Nonetheless, expanded porphyrins receive much attention in the state-of-the-art research, due to their potential in supramolecular photo electronics.<sup>[7]</sup>

For host-guest interactions of curved molecules a concave structure is preferred, especially for the binding of fullerenes. But also fullerene peapods, like carbon nanotubes and macrocycles consisting of aryl or heteroaryl as well as organometallic

moieties are known.<sup>[8]</sup> Recently, a molecular nanobarrel was reported to host C<sub>60</sub>.<sup>[9]</sup>

Porphyrins and their expanded derivatives often have a flat, twisted or band-like morphology, which is less suitable for molecular interactions with a ball-shaped molecule like fullerene<sup>[10]</sup> that prefers a host molecule of a concave design.<sup>[5]</sup> To realize a suitable binding site for fullerenes nonetheless, aromatic substituents and additional concave structures have been added.<sup>[11]</sup> Polycyclic hydrocarbon cores are used in the design of a “buckycatcher” by Sygula, Álvarez, and Torroba with two or four attached corannulene moieties in a tweezer-like conformation fitting perfectly one and two fullerenes respectively.<sup>[12]</sup> Another novel approach is to modify the molecule in such a way that it obtains a concave shape. This can be achieved by introducing strain, like in corannulene derivatives<sup>[13]</sup> or even bigger rings, gaining a bowl- or saddle shaped structure.<sup>[6,14]</sup>

In the following we report on an expanded porphyrinoid macrocycle with a saddle shape morphology that is suitable to host fullerene by  $\pi$ - $\pi$  interactions.

## Results and Discussion

Previously, we reported the synthesis of a carbenaporphyrin ligand.<sup>[15]</sup> In the key step of its synthesis, the macrocyclization via a copper catalyzed azide alkyne cycloaddition (CuAAC, click reaction), we recognized the formation of side product (Scheme 1). Like the main product **1**, the <sup>1</sup>H NMR spectrum of the isolated side product shows seven characteristic signals in the aromatic region, which are however, shifted over a broader chemical shift range. Mass spectrometry reveals the main signal at  $m/z = 1378.8$ , which corresponds to twice the mass of the main macrocycle **1** ( $[M + H]^+$ ). Therefore, we identified it as the macrocycle **2** that is formed from two moieties of each the carbazolyl dialkyne and the carbazolyl diazide substrate. We could improve the formation of this colorless macrocycle **2** to up to 23% isolated yield by increasing the substrate concentration in the click reaction. Since we still need **1**, we obtained

[a] T. Maulbetsch, Prof. Dr. D. Kunz  
Institut für Anorganische Chemie  
Eberhard Karls Universität Tübingen  
Auf der Morgenstelle 18, 72076 Tübingen (Germany)  
E-mail: Doris.Kunz@uni-tuebingen.de  
Homepage: <http://www.uni-tuebingen.de/kunz>

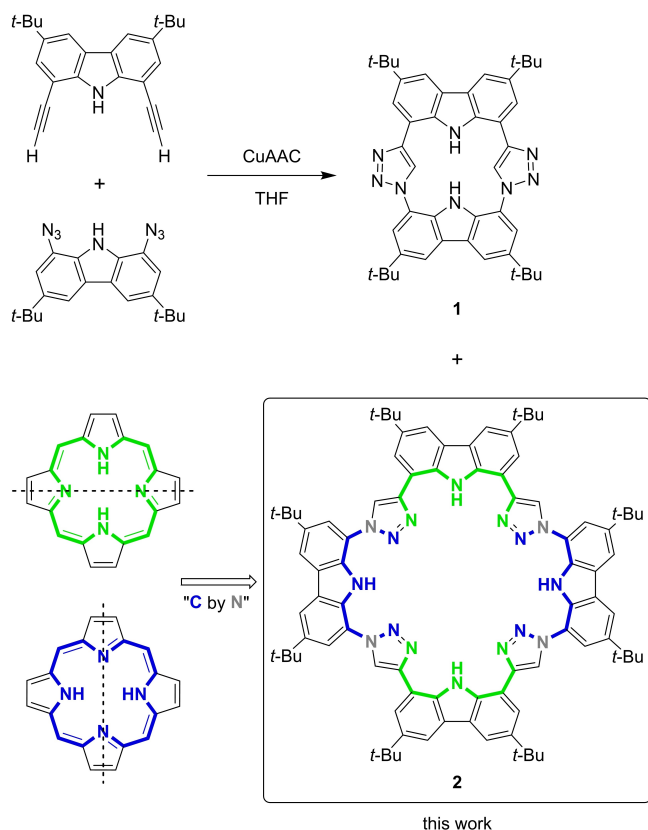
[b] P. Frech, Prof. Dr. M. Scheele  
Institut für Physikalische Chemie und Theoretische Chemie  
Eberhard Karls Universität Tübingen  
Auf der Morgenstelle 18, 72076 Tübingen (Germany)

[c] Prof. Dr. K. W. Törnroos  
Department of Chemistry  
University of Bergen  
5007 Bergen (Norway)

[\*\*] A previous version of this manuscript has been deposited on a preprint server (<https://chemrxiv.org/engage/chemrxiv/article-details/64052ab937e01856dc3574ea>).

Supporting information for this article is available on the WWW under <https://doi.org/10.1002/chem.202302104>

© 2023 The Authors. Chemistry - A European Journal published by Wiley-VCH GmbH. This is an open access article under the terms of the Creative Commons Attribution Non-Commercial NoDerivs License, which permits use and distribution in any medium, provided the original work is properly cited, the use is non-commercial and no modifications or adaptations are made.



**Scheme 1.** Synthesis of **1** and **2** via a CuAAC click reaction and illustration of the construction of the expanded porphyrin **2** by formal annulation of two bisected porphyrins (and substitution of four C atoms by N) as building blocks.

enough of **2** so that further optimization of the selectivity of the reaction towards **2** is not necessary at this stage.

The  $^1\text{H}$  NMR spectrum is consistent with a  $C_{2v}$  symmetric macrocycle. At 11.87 and 10.75 ppm two signals for the chemically different carbazole NH-protons can be observed. The triazole has a distinct signal at 8.80 ppm leaving the four aromatic signals of the carbazole protons as doublets between 8.5 and 7.7 ppm. Additionally, two signals at 1.54 and 1.46 ppm are detected with an integral of each 36H for the two inequivalent *tert*-butyl groups.

The macrocyclic framework consists only of  $sp^2$  hybridized carbon and nitrogen atoms. All nitrogen atoms are situated on the inner ring, which results in four NNN-pincer-like pockets (Scheme 1) that can be regarded as half a porphyrin each. Merging (and formal substitution of C by N) forms a so-called expanded porphyrin with 36 atoms in the inner ring. The NNN-pincer moieties could be additionally functionalized by metal complexation.

The optical properties of **2** in THF were studied by steady-state UV/vis absorption and -fluorescence spectroscopy, as well as transient absorption spectroscopy (Figure 1). We observe a first absorption band with maxima at 373 and 357 nm followed by a second, larger band at 298 nm. Upon excitation at 305 nm, we detect a narrow fluorescence maximum at 383 nm as well as a broader signal at 400 nm with a tailing shoulder at 425 nm

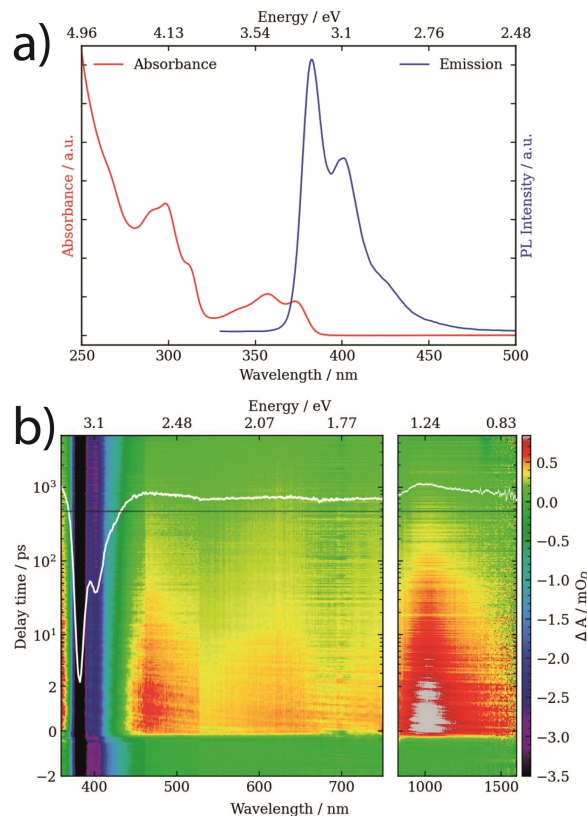


**Figure 1.** Optical properties of **2** in THF: a) Normalized steady-state absorption (red) and fluorescence (blue) spectra. b) UV/vis/NIR transient absorption spectrum after 350 nm excitation within a spectral window of 350 nm–1600 nm and a pump-probe delay of 150 fs–8 ns. The color code on the right refers to the magnitude and sign of the differential absorption (excited state - ground state). The white solid line exemplifies the transient absorption spectrum after 1 ps in arbitrary units.

and a fluorescence quantum yield of 60%. For comparison, we note that the dimeric macrocycle **1** exhibits similar, hypsochromically shifted spectral features (first absorption/fluorescence maximum at 360 nm/378 nm) with roughly half the reported quantum yield of **2**.<sup>[16]</sup>

UV/vis/NIR transient absorption spectroscopy of **2** in THF following 90 fs pump pulses at 350 nm (1  $\mu\text{J}/\text{pulse}$ ) shows the expected ground-state bleach as well as broad excited-state absorption centered at 445 nm, 620 nm, and 1020 nm. All three features exhibit similar exponential decay kinetics, which can be fit with two short lifetime components on the order of 10 ps and 200 ps as well as one long-lived process on the order of 8 ns. We note that the strong excited-state absorption at 1020 nm is reminiscent of other porphyrinoids,<sup>[17]</sup> where it has been ascribed to a transition from the  $S_1$  excited state to the  $1^1E_g$  state.<sup>[18]</sup> In contrast to such classical porphyrinoid features, we do not observe a significant Q-band or any long-lived transitions at a pump-probe delay  $\geq 10$  ns, which would be indicative of intersystem crossing into a triplet state.

DFT and TD-DFT calculations show similar molecular orbitals and electronic transitions of **1** and **2**, with the molecular orbitals being mostly localized on one aromatic moiety and, in the case of **2**, also on opposite moieties. Macrocycle **2** has twice the

number of aromatic moieties and thus, twice the number of MOs that mostly are pairs of spatially and energetically similar orbitals originating from the symmetric nature of the macrocycle. Consequently, this leads to energetically closer electronic transitions, which can be recognized from the UV/VIS spectrum via a smaller distance of the bands (see Supporting Information for more details).

Single crystals suitable for X-ray diffraction could be obtained from a supersaturated solution of **2** in acetonitrile. The solid-state molecular structure confirms the tetrameric nature consisting of four carbazole moieties linked by four triazole moieties (Figure 2). The carbazole moieties are connected pairwise either to the N or the C atom of the triazole, which is however, not resolved in the crystal structure due to a stoichiometric disorder of the triazole nitrogen and carbon positions. In the crystal, one carbazole moiety is  $\pi$ -stacked antiparallel to the carbazole moiety of a second molecule with an interplanar distance of 3.79 Å.

Within the four NNN-pincer-like pockets, the carbazole nitrogen atoms are 2.9 Å apart from the respective triazole nitrogen atoms, which are 4.3 Å apart from each other (mean

values). This resembles the distances in porphyrin derivatives, for example, porphyrin with 2.889 Å and 4.112 Å respectively.

The alternating linkage of the carbazole and triazole moieties leads to a strain in the macrocycle that is reduced by adopting a saddle-shaped conformation. The carbazole moieties at opposite sides are tilted pairwise by 80° and 95° against each other. We attribute the difference to packing effects and the mentioned intermolecular  $\pi$ -interaction of one carbazole moiety in the solid state. This is reasonable as DFT calculations in the gas phase show a smaller difference of this tilting (93° for the N-bonded and 90° for the C-bonded carbazole planes). The saddle shape of **2** results in two concave cavities, with a mean distance between the two symmetry-equivalent carbazole moieties in the solid-state structure of 11 Å (measured from the carbazole centers). The height of each cavity, determined from the center of the molecule to the plane spanned by the tertiary carbons of the corresponding *tert*-butyl groups measures 4.4 Å. Such large voids spanned by an extended  $\pi$ -system can be very useful in host-guest complexation. With its large aromatic system and the perfect diameter of about 10 Å, the C<sub>60</sub> fullerene is a promising candidate to form a host-guest complex with potentially interesting properties.<sup>[19]</sup>

Addition of C<sub>60</sub> to macrocycle **2** in toluene-d<sub>8</sub> shows clear signs of a host-guest interaction by distinct shifts of <sup>1</sup>H NMR signals: The signals of the *t*-Bu groups shift from 1.354 to 1.377 ppm and 1.509 to 1.531 ppm upon titration with 5 equiv. of C<sub>60</sub> (Figure 3). The aromatic signals show a similar down-field

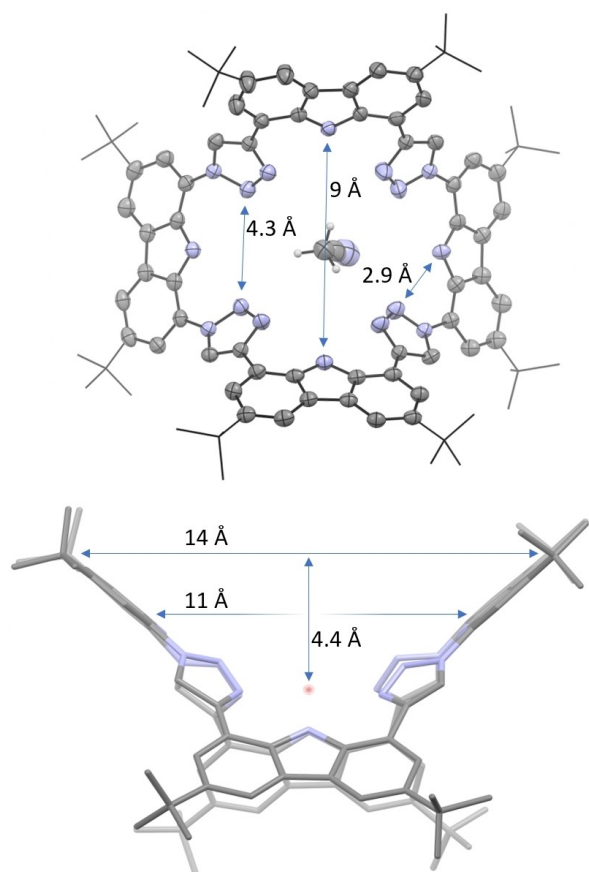


**Figure 2.** Top: Solid-state molecular structure of macrocycle **2** hosting one acetonitrile molecule in the central cavity (anisotropic atomic displacement parameters at the 50% probability level). For clarity, *tert*-Bu moieties are shown with wireframe. Bottom: Wireframe side view of macrocycle **2**. Hydrogen atoms and co-crystallized acetonitrile molecules are omitted. All distances are displayed as mean values.

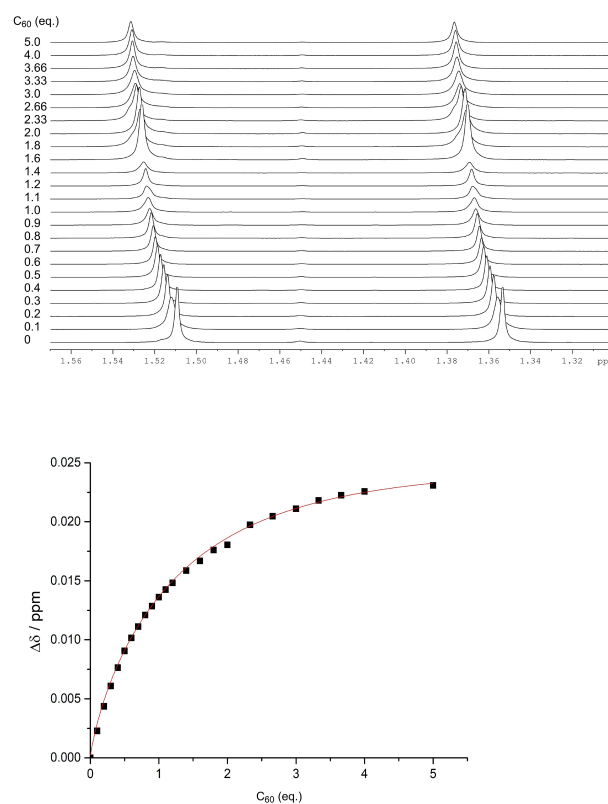


**Figure 3.** Titration of **2** in toluene-d<sub>8</sub> (4.3 mM) with C<sub>60</sub> in toluene-d<sub>8</sub> (2.8 mM) followed by <sup>1</sup>H NMR spectroscopy (400 MHz): shift of the *t*-Bu signals (top) and correlation between the shift difference of the *t*-Bu signal at 1.35 ppm and the amount of added fullerene (concentration of **2** not constant).

shift of about 0.02 ppm each. The concentration of **2** was not kept constant, however, a mere concentration effect on the chemical shift due to the titration can be excluded as diluting a solution of pure **2** in toluene- $d_8$  causes no change of the NMR spectrum. The result shows qualitatively that the binding affinity is rather low.

In contrast to the good detectability by NMR spectroscopy, the host–guest complexation could neither be detected in the UV/VIS nor in the fluorescence spectra. Optical spectroscopy requires significantly lower concentrations (0.5–30  $\mu\text{M}$ ) than the aforementioned NMR experiments (4 mM) in order to maintain sufficient transmission and/or prevent reabsorption. Due to the low binding constant, the strong dilution hampers the formation of the host–guest interaction. The IR (ATR) spectrum of the host–guest complex shows no significant difference compared to the superimposed spectra of the starting materials **2** and  $\text{C}_{60}$ .

Nonetheless, from a saturated solution in toluene it was possible to grow single crystals suitable for X-ray diffraction by diffusion of methanol. Despite their weak diffraction, we could

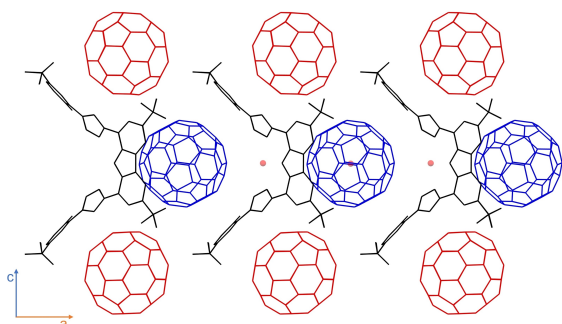


**Figure 4.** The solid-state molecular structure of the host–guest complex  $2 \cdot (\text{C}_{60})_4$  between **2** (black) and  $\text{C}_{60}$  (view along the  $b$ -axis; blue:  $\text{C}_{60}$  along the ligand chain; red: lateral  $\text{C}_{60}$ ). For clarity, all molecules are shown using wireframes, and hydrogen atoms as well as a third type of  $\text{C}_{60}$  (see Figure 5) are omitted. The red dot marks the center of **2** and of one fullerene.

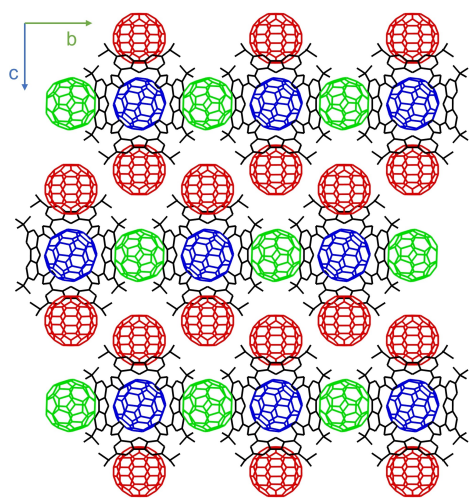


**Figure 5.** View along the  $a$ -axis of the solid-state structure of the host–guest complex  $2(\text{C}_{60})_4$  between **2** (black) and  $\text{C}_{60}$  (blue: in the coordination polymer strain; red and green: lateral). All molecules are shown as wireframe, and hydrogen atoms are omitted for clarity.

obtain the molecular structure (Figures 4 and 5) of the host–guest complex between macrocycle **2** and  $\text{C}_{60}$ .

The fullerene interacts not only with the aromatic carbazole  $\pi$ -system in the concave confinement on both sides of each carbazole, but also at the exterior side of each carbazole moiety resulting in a 4:1 ratio of fullerene to **2**. The core of the structure  $2 \cdot (\text{C}_{60})_4$  consists of a polymeric chain, in which one type of fullerenes (Figure 4, blue) is encapsulated by the concave shell of two macrocycles. Thus, this  $\text{C}_{60}$  is coordinated by four carbazole moieties from two different macrocycles in a tetrahedral manner. Only a handful of similar host–guest structures are known<sup>[3b,6,20]</sup> with even fewer forming columns of alternating host–guest complexes.<sup>[5,21]</sup> The remaining concave shell of each macrocycle is also occupied by fullerene in the same manner, thus forming a one-dimensional coordination polymer. This polymer strand is flanked by additional fullerenes coordinated to the lateral  $\pi$ -system of each carbazole moiety which forms additional concave confinements by London dispersion with the *tert*-butyl groups of the two adjacent carbazole moieties. This leads to the second type of fullerene that is coordinated along the  $c$ -axis of the unit cell (marked in red) and requires two fullerenes per macrocycle. For the third type of fullerene (Figure 5, green) the flanking fullerene interconnects two polymer strands. The host macrocycle shows an inclination of the carbazole planes of  $71^\circ$  and  $95^\circ$  which reveals that hardly any conformational change in the free macrocycle **2** ( $80^\circ$  and  $95^\circ$ ) is necessary for the complexation of the fullerenes. The slightly different angles also result in slightly different distances between the center of **2** and the two coordinated  $\text{C}_{60}$  in the  $a$ -direction of 6.9 and 6.7  $\text{\AA}$  measured from their centroids. Thus, the  $\text{C}_{60}$ – $\text{C}_{60}$  distance through the macrocycle measures 13.6  $\text{\AA}$ , which is slightly longer than in the alternating complex between  $\text{C}_{60}$  and an extended phthalocyanine (12.7  $\text{\AA}$ ).<sup>[5]</sup> In the geometrically more related thiacalix[4]DTT host–guest complex the fullerenes are only slightly further apart (10.3  $\text{\AA}$ ) than in pure  $\text{C}_{60}$  crystals (10.0  $\text{\AA}$ ), which is a consequence of the less rigid binding pocket of that host.<sup>[6,19]</sup>

## Conclusions

In conclusion, we synthesized an expanded,  $\pi$ -extended porphyrinoid that exhibits a violet-blue fluorescence with 60% quantum yield. Its unique  $\pi$ -conjugated saddle-shaped geometry results in two bowl-shaped confinements of 11  $\text{\AA}$  which are suitable for accommodating  $\text{C}_{60}$ . The complexation of  $\text{C}_{60}$  is realized by  $\pi$ – $\pi$  interactions as well as London dispersions. This results in a one-dimensional coordination polymer whose strands are further connected by lateral coordinated fullerenes. Besides the possibility of hosting other convex molecules, an additional feature of our macrocycle **2** are the NNN-pincer moieties that could be further functionalized, for example, by complexation of metal ions. This could make this new macrocycle an interesting ligand for combining both host–guest interactions and coordination chemistry.

## Experimental Section

**General Information:** Unless otherwise stated, all reactions were carried out under an argon atmosphere in dried and degassed solvents using Schlenk technique. Toluene, tetrahydrofuran, dichloromethane, and diethyl ether were dried using an MBraun SPS-800 solvent purification system. Deuterated solvents were dried with standard purification methods and degassed.<sup>[22]</sup> The precursors 3,6-di-*tert*-butyl-carbazole<sup>[23]</sup> and 1,8-diethynyl-3,6-di-*tert*-butyl-carbazole<sup>[24]</sup> were synthesized according to the literature. Supporting Information contains the numbering scheme for the NMR peak assignment.

CCDC Deposition Number(s) 2245615 (Macrocycle2) and 2245616 (Complex2) contain(s) the supplementary crystallographic data for this paper. These data are provided free of charge by the joint Cambridge Crystallographic Data Centre and Fachinformationszentrum Karlsruhe Access Structures service.

**Synthesis of macrocycle 2:** In a modification of the procedure described earlier,<sup>[15]</sup> a round bottom flask with 1,8-diazido-3,6-di-*tert*-butyl-carbazole (1.00 g, 2.77 mmol, 1 eq), 1,8-diethynyl-3,6-di-*tert*-butyl-carbazole (906 mg, 2.77 mmol, 1 eq) copper sulfate pentahydrate (69.0 mg, 277  $\mu$ mol, 0.1 eq), TBTA (155 mg, 277  $\mu$ mol, 0.1 eq) and sodium ascorbate (274 mg, 1.38 mmol, 0.3 eq) were put under argon. 500 mL of degassed tetrahydrofuran and triethylamine (2.88 mL) were added. The flask was sealed and heated to 60 °C under stirring for 3 d. After filtration and concentration of the suspension in vacuo to 18 g, 40 mL of methanol were added, and the precipitate was filtered off and washed with two times 4 mL of methanol to yield 440 mg (23%) of the small macrocycle 1 as a white solid. The solution was then concentrated to half the volume to precipitate the raw product of 2 overnight, which was filtered off and eluted over silica gel with diethyl ether. The eluate was washed with pentane and dried in vacuo to yield macrocycle 2 (430 mg, 23%) as an off-white solid.

**<sup>1</sup>H NMR** (THF-*d*<sub>6</sub>, 500.11 MHz)  $\delta$  11.87 (s, 2H, H-19), 10.75 (s, 2H, H-9), 8.80 (s, 4H, H-5'), 8.46 (d, <sup>4</sup>J<sub>HH</sub> = 1.7 Hz, 4H, H-4), 8.15 (d, <sup>4</sup>J<sub>HH</sub> = 1.8 Hz, 4H, H-14), 7.82 (d, <sup>4</sup>J<sub>HH</sub> = 1.7 Hz, 4H, H-12), 7.78 (d, <sup>4</sup>J<sub>HH</sub> = 1.8 Hz, 4H, H-2), 1.54 (s, 36H; H-21), 1.46 (s, 36H; H-25). **<sup>1</sup>H NMR** (toluene-*d*<sub>6</sub>, 400.11 MHz)  $\delta$  12.25 (s, 2H, NH), 10.75 (s, 2H, NH), 8.40 (d, <sup>4</sup>J<sub>HH</sub> = 1.5 Hz, 4H, Ar-H), 8.26 (d, <sup>4</sup>J<sub>HH</sub> = 1.5 Hz, 4H, Ar-H), 7.83 (s, 4H, H-5'), 7.69 (d, <sup>4</sup>J<sub>HH</sub> = 1.8 Hz, 4H, Ar-H), 7.31 (d, <sup>4</sup>J<sub>HH</sub> = 1.8 Hz, 4H, Ar-H), 1.51 (s, 36H, t-Bu), 1.36 (s, 36H, t-Bu). **<sup>13</sup>C NMR** (THF-*d*<sub>6</sub>, 125.11 MHz)  $\delta$  148.7 (C4'), 144.2 (C3), 142.5 (C13), 136.9 (C14a), 134.5 (C4a), 126.9 (C1), 125.2 (C11), 123.2 (C1a), 122.3 (C5'), 121.6 (C12), 120.7 (C2), 118.8 (C4), 117.0 (C14), 114.3 (C11a), 35.8 (C20), 35.5 (C24), 32.6 (C25), 32.4 (C21). **ESI<sup>+</sup>**: (MeCN) 1378.81 [M + H]<sup>+</sup>, 689.93 [M + 2H]<sup>2+</sup>. **IR:** (ATR) 3419, 2959, 2901, 2869, 1598, 1487, 1433, 1363, 1290, 1175, 1037, 869, 785, 672, 651, 608 cm<sup>-1</sup>.

**Synthesis of the host-guest complex 2\*(C<sub>60</sub>)<sub>4</sub>:** A solution of 2 (4.0 mg, 2.9  $\mu$ mol, 1 eq) in 0.2 mL toluene was added to a solution of C<sub>60</sub> (4.2 mg, 5.8  $\mu$ mol, 2 eq) in 2.0 mL toluene. After diffusion of methanol into the solution large crystals of the host-guest complex 2\*(C<sub>60</sub>)<sub>4</sub> could be obtained, which reveals a stoichiometry in the crystal of 2:C<sub>60</sub> = 1:4.<sup>[25]</sup>

## Supporting Information

The Supporting Information contains NMR, IR and UV spectra, information on the X-ray structure analyses<sup>[25]</sup> as well as the DFT calculation results. The authors have cited additional references within the Supporting Information.<sup>[26–32]</sup>

## Acknowledgements

T.M. thanks the MWK-BW for a fellowship (Landesgraduiertenförderung). We acknowledge Dilan Ehrlich, Ruslan Jaufmann and Cornelia Helena Warmutz for help with synthesis. The TA measurements were funded by the DFG under contract INST 37/1160-1 FUGG (project nr. 458406921). Open Access funding enabled and organized by Projekt DEAL.

## Conflict of Interests

The authors declare no conflict of interest.

## Data Availability Statement

The data that support the findings of this study are available in the supplementary material of this article.

**Keywords:** carbazole · expanded porphyrinoids · fullerenes · host-guest · macrocycles

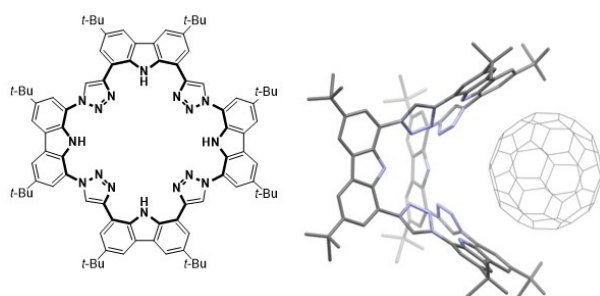
- [1] J. L. Sessler, A. K. Burrell in *Macrocycles. With 10 tables, Topics in Current Chemistry, Vol. 161*; (Ed. E. Weber), Springer, Berlin, 1992, pp. 177–273.
- [2] a) A. Srinivasan, T. Ishizuka, A. Osuka, H. Furuta, *J. Am. Chem. Soc.* **2003**, *125*, 878–879; b) A. Alka, V. S. Shetti, M. Ravikanth, *Coord. Chem. Rev.* **2019**, *401*, 213063.
- [3] a) A. Jana, M. Ishida, H. Furuta, *Chem. Eur. J.* **2021**, *27*, 4466–4472; b) N. J. Tremblay, A. A. Gorodetsky, M. P. Cox, T. Schiros, B. Kim, R. Steiner, Z. Bullard, A. Sattler, W.-Y. So, Y. Itoh, M. F. Toney, H. Ogasawara, A. P. Ramirez, I. Kymissis, M. L. Steigerwald, C. Nuckolls, *ChemPhysChem* **2010**, *11*, 799–803.
- [4] A. Srinivasan, V. M. Reddy, S. J. Narayanan, B. Sridevi, S. K. Pushpan, M. Ravikumar, T. K. Chandrashekar, *Angew. Chem. Int. Ed.* **1997**, *36*, 2598–2601.
- [5] S. Shimizu, A. Miura, N. Kobayashi, *CrystEngComm* **2013**, *15*, 3759.
- [6] R. Inoue, M. Hasegawa, T. Nishinaga, K. Yoza, Y. Mazaki, *Angew. Chem. Int. Ed.* **2015**, *54*, 2734–2738.
- [7] a) A. D. Bromby, D. T. Hogan, T. C. Sutherland, *New J. Chem.* **2017**, *41*, 4802–4805; b) D. M. Guldi, *Chem. Soc. Rev.* **2002**, *31*, 22–36.
- [8] a) B. W. Smith, M. Monthieux, D. E. Luzzi, *Nature* **1998**, *396*, 323–324; b) T. Kawase, M. Oda, *Pure Appl. Chem.* **2006**, *78*, 831–839; c) S. Toyota, M. Goichi, M. Kotani, *Angew. Chem. Int. Ed.* **2004**, *43*, 2248–2251; d) H. Shimizu, J. D. Cojal González, M. Hasegawa, T. Nishinaga, T. Haque, M. Takase, H. Otani, J. P. Rabe, M. Iyoda, *J. Am. Chem. Soc.* **2015**, *137*, 3877–3885; e) T. Iwamoto, Y. Watanabe, T. Sadahiro, T. Haino, S. Yamago, *Angew. Chem. Int. Ed.* **2011**, *50*, 8342–8344; f) T. Kawase, K. Tanaka, Y. Seirai, N. Shiono, M. Oda, *Angew. Chem. Int. Ed.* **2003**, *42*, 5597–5600; g) Y. Yamamoto, E. Tsurumaki, K. Wakamatsu, S. Toyota, *Angew. Chem. Int. Ed.* **2018**, *57*, 8199–8202; h) V. Martínez-Agramunt, T. Eder, H. Darmandeh, G. Guisado-Barrios, E. Peris, *Angew. Chem. Int. Ed.* **2019**, *58*, 5682–5686; i) S. Lampart, L. M. Roch, A. K. Dutta, Y. Wang, R. Warshamanage, A. D. Finke, A. Linden, K. K. Baldrige, J. S. Siegel, *Angew. Chem. Int. Ed.* **2016**, *55*, 14648–14652.
- [9] S. Bera, S. Das, M. Melle-Franco, A. Mateo-Alonso, *Angew. Chem. Int. Ed.* **2023**, *62*, e202216540.
- [10] a) R. Misra, T. K. Chandrashekar, *Acc. Chem. Res.* **2008**, *41*, 265–279; b) S. Saito, A. Osuka, *Angew. Chem. Int. Ed.* **2011**, *50*, 4342–4373.
- [11] a) S. Ferrero, H. Barbero, D. Miguel, R. García-Rodríguez, C. M. Álvarez, *J. Org. Chem.* **2020**, *85*, 4918–4926; b) S. Ferrero, H. Barbero, D. Miguel, R. García-Rodríguez, C. M. Álvarez, *RSC Adv.* **2020**, *10*, 36164–36173; c) Y. Xu, S. Gsänger, M. B. Minameyer, I. Imaz, D. Maspocho, O. Shyshov, F. Schwer, X. Ribas, T. Drewello, B. Meyer, M. von Delius, *J. Am. Chem. Soc.* **2019**, *141*, 18500–18507.
- [12] a) A. Sygula, F. R. Fronczek, R. Sygula, P. W. Rabideau, M. M. Olmstead, *J. Am. Chem. Soc.* **2007**, *129*, 3842–3843; b) V. García-Calvo, J. V. Cuevas, H.

- Barbero, S. Ferrero, C. M. Álvarez, J. A. González, B. Díaz de Greñu, J. García-Calvo, T. Torroba, *Org. Lett.* **2019**, *21*, 5803–5807; c) C. M. Álvarez, L. A. García-Escudero, R. García-Rodríguez, J. M. Martín-Álvarez, D. Miguel, V. M. Rayón, *Dalton Trans.* **2014**, *43*, 15693–15696; d) A. Sygula, *Synlett* **2016**, *27*, 2070–2080; e) M. Yanney, F. R. Fronczek, A. Sygula, *Angew. Chem. Int. Ed.* **2015**, *54*, 11153–11156; f) C. M. Álvarez, G. Aullón, H. Barbero, L. A. García-Escudero, C. Martínez-Pérez, J. M. Martín-Álvarez, D. Miguel, *Org. Lett.* **2015**, *17*, 2578–2581.
- [13] a) Y. Sasaki, M. Takase, N. Kobayashi, S. Mori, K. Ohara, T. Okujima, H. Uno, *J. Org. Chem.* **2021**, *86*, 4290–4295; b) D. Sepúlveda, Y. Guan, U. Rangel, S. E. Wheeler, *Org. Biomol. Chem.* **2017**, *15*, 6042–6049.
- [14] X.-S. Ke, T. Kim, J. T. Brewster, V. M. Lynch, D. Kim, J. L. Sessler, *J. Am. Chem. Soc.* **2017**, *139*, 4627–4630.
- [15] T. Maulbetsch, D. Kunz, *Angew. Chem. Int. Ed.* **2021**, *60*, 2007–2012.
- [16] L. Arnold, PhD thesis, Johannes Gutenberg-Universität Mainz, **2012**.
- [17] D. B. Moravec, B. M. Lovaasen, M. D. Hopkins, *J. Photochem. Photobiol. A* **2013**, *254*, 20–24.
- [18] O. Schalk, H. Brands, T. S. Balaban, A.-N. Unterreiner, *J. Phys. Chem. A* **2008**, *112*, 1719–1729.
- [19] O. A. Dyachenko, A. Graja, *Fullerene Sci. Technol.* **1999**, *7*, 317–385.
- [20] D. P. Sumy, N. J. Dodge, C. M. Harrison, A. D. Finke, A. C. Whalley, *Chem. Eur. J.* **2016**, *22*, 4709–4712.
- [21] a) Z. Wang, F. Dötz, V. Enkelmann, K. Müllen, *Angew. Chem. Int. Ed.* **2005**, *44*, 1247–1250; b) Y. Yang, K. Cheng, Y. Lu, D. Ma, D. Shi, Y. Sun, M. Yang, J. Li, J. Wei, *Org. Lett.* **2018**, *20*, 2138–2142.
- [22] W. L. F. Armarego, C. L. L. Chai, *Purification of laboratory chemicals*; Butterworth-Heinemann, Amsterdam, Heidelberg, **2009**.
- [23] Y. Liu, M. Nishiura, Y. Wang, Z. Hou, *J. Am. Chem. Soc.* **2006**, *128*, 5592–5593.
- [24] M. S. Bennington, H. L. C. Feltham, Z. J. Buxton, N. G. White, S. Brooker, *Dalton Trans.* **2017**, *46*, 4696–4710.
- [25] Deposition numbers 2245615 (for **2**) and 2245616 (for **2**\*(C<sub>60</sub>)<sub>4</sub>) contain the supplementary crystallographic data for this paper. These data are provided free of charge by the joint Cambridge Crystallographic Data Centre and Fachinformationszentrum Karlsruhe Access Structures service.
- [26] G. M. Sheldrick, SADABS 2012/1; University of Göttingen, Göttingen, Germany, **2012**.
- [27] a) G. M. Sheldrick, *Acta Crystallogr.* **2008**, *A64*, 112–122; b) G. M. Sheldrick, *Acta Crystallogr.* **2015**, *C71*, 3–8; c) C. B. Hübschle, G. M. Sheldrick, B. Dittrich, *J. Appl. Crystallogr.* **2011**, *44*, 1281–1284; d) G. M. Sheldrick, *Acta Crystallogr.* **2015**, *A71*, 3–8.
- [28] a) F. Neese, *WIREs Comput. Mol. Sci.* **2018**, *8*:e 1327; b) F. Neese, F. Wennmohs, U. Becker, C. Riplinger, *J. Chem. Phys.* **2020**, *152*, 224108.
- [29] a) F. Weigend, *Phys. Chem. Chem. Phys.* **2002**, *4*, 4285–4291; b) F. Neese, F. Wennmohs, A. Hansen, U. Becker, *Chem. Phys.* **2009**, *356*, 98–109; c) S. Kossmann, F. Neese, *Chem. Phys. Lett.* **2009**, *481*, 240–243.
- [30] a) A. D. Becke, *Physical Rev. A* **1988**, *38*, 3098–3100; b) J. P. Perdew, *Phys. Rev. B* **1986**, *33*, 8822–8824; c) C. Lee, W. Yang, R. G. Parr, *Phys. Rev. B* **1988**, *37*, 785–789; d) S. Grimme, S. Ehrlich, L. Goerigk, *J. Comput. Chem.* **2011**, *32*, 1456–1465; e) S. Grimme, J. Antony, S. Ehrlich, H. Krieg, *J. Chem. Phys.* **2010**, *132*, 154104; f) F. Weigend, R. Ahlrichs, *Phys. Chem. Chem. Phys.* **2005**, *7*, 3297–3305.
- [31] F. Neese, G. Olbrich, *Chem. Phys. Lett.* **2002**, *362*, 170–178.
- [32] A. Rüütel, V. Yrjänä, S. A. Kadam, I. Saar, M. Ilisson, A. Darnell, K. Haav, T. Haljasorg, L. Toom, J. Bobacka, I. Leito, *Beilstein J. Org. Chem.* **2020**, *16*, 1901–1914.

Manuscript received: July 2, 2023

Accepted manuscript online: July 8, 2023

Version of record online: ■ ■ ■



**A saddle-shaped macrocyclic host:**  
An expanded porphyrinoid macrocycle with a saddle-shaped structure was synthesized. It is suitable for host-guest complexation by  $\pi$ - $\pi$  interactions with four equivalents of

fullerene C<sub>60</sub> in all three directions. UV/vis/NIR transient absorption spectroscopy exhibits a strong long-lived NIR absorption reminiscent of that of porphyrins but shows no porphyrin-type Q-band.

*T. Maulbetsch, P. Frech, Prof. Dr. M. Scheele, Prof. Dr. K. W. Törnroos, Prof. Dr. D. Kunz\**

1 – 7

**A Saddle-Shaped Expanded Porphyrinoid Fitting C<sub>60</sub>**

